PCCP

PAPER

Dynamics of the D^+ + H_2 and H^+ + D_2 reactions: a detailed comparison between theory and experiment

P. G. Jambrina,[ab] J. M. Alvariño,[b] D. Gerlich,[c] M. Hankel,[d] V. J. Herrero,*[e] V. Sáez-Rábanos[f] and F. J. Aoiz*[a]

An extensive set of experimental measurements on the dynamics of the H^+ + D_2 and D^+ + H_2 ion–molecule reactions is compared with the results of quantum mechanical (QM), quasiclassical trajectory (QCT), and statistical quasiclassical trajectory (SQCT) calculations. The dynamical observables considered include specific rate coefficients as a function of the translational energy, E_T, thermal rate coefficients in the 100–500 K temperature range. In addition, kinetic energy spectra (KES) of the D^+ ions reactively scattered in H^+ + D_2 collisions are also presented for translational energies between 0.4 eV and 2.0 eV. For the two reactions, the best global agreement between experiment and theory over the whole energy range corresponds to the QCT calculations using a Gaussian binning (GB) procedure, which gives more weight to trajectories whose product vibrational action is closer to the actual integer QM values. The QM calculations also perform well, although somewhat worse over the more limited range of translational energies where they are available ($E_T < 0.6$ eV and $E_T < 0.2$ eV for the H^+ + D_2 and D^+ + H_2 reactions, respectively). The worst agreement is obtained with the SQCT method, which is only adequate for low translational energies. The comparison between theory and experiment also suggests that the most reliable rate coefficient measurements are those obtained with the merged beams technique. It is worth noting that none of the theoretical approaches can account satisfactorily for the experimental specific rate coefficients of H^+ + D_2 for $E_T \leq 0.2$ eV although there is a considerable scatter in the existing measurements. On the whole, the best agreement with the experimental laboratory KES is obtained with the simulations carried out using the state resolved differential cross sections (DCSs) calculated with the QCT-GB method, which seems to account for most of the observed features. In contrast, the simulations with the SQCT data predict kinetic energy spectra (KES) considerably cooler than those experimentally determined.

I. Introduction

Gas-phase chemical reactions involving ionic species are, in general, more easily amenable to experimental investigation than those implying only neutrals, given the inherent advantages for ion preparation, manipulation and detection.

[a] Departamento de Química Física, Facultad de Química, Universidad Complutense, 28040 Madrid, Spain. E-mail: aoiz@quim.ucm.es
[b] Grupo de Dinámica Molecular, Departamento de Química Física, Facultad de Ciencias Químicas, Universidad de Salamanca, 37008 Salamanca, Spain
[c] Institute of Physics, University of Technology, 09107 Chemnitz, Germany
[d] Centre for Computational Molecular Science, Australian Institute for Bioengineering and Nanotechnology, The University of Queensland, Qld 4072, Brisbane, Australia
[e] Instituto de Estructura de la Materia (CSIC), Serrano 123, 28006 Madrid, Spain. E-mail: v.herrero@csic.es
[f] Departamento de Química y Bioquímica, ETS Ingenieros de Montes, Universidad Politécnica, 28040 Madrid, Spain

Consequently, a large number of kinetic data for ion–molecule reactions has been obtained over decades with a variety of experimental procedures including bulk-phase methods, beam techniques, and ion-traps.[1–14] Depending on the system, the experimental data currently available range from thermally averaged rate coefficients, $k(T)$, *via* state specific cross sections to state-resolved differential cross sections (DCS). Quite commonly, reactions of ions with neutrals do not have a significant barrier and due to their long range attractive potentials exhibit large cross sections. This renders them especially relevant at the low temperatures typical of the interstellar medium (see ref. 15–17 and references therein). In the past decades, much experimental effort has been dedicated to extend the temperature range down to a few K. The difficulties associated with the handling of small relative translational energies, E_T, in ion–molecule reactions have been overcome through the use of supersonic jets,[5,8,13,14] guided and merged beams, and ion traps.[1,9–12] A great variety of processes ranging from simple

3346 | *Phys. Chem. Chem. Phys.*, 2012, **14**, 3346–3359

This journal is © the Owner Societies 2012

elastic and inelastic cross sections for the triatomic A + BC system to reactive processes and the formation or destruction of polyatomic molecules and clusters have been studied in these experiments. In particular, special attention has been paid to the study of hydrogenic ions and specifically to the investigation of the H_3^+ system.

The H_3^+ molecule is the most abundant triatomic ionic species in dense interstellar clouds[18] and in many cold hydrogen plasmas.[19,20] This ion is also formed as a strongly bound intermediate in collisions of H^+ with H_2. Due to its apparent simplicity, this system constitutes a prototype in the field of ion–molecule reactions and as such has been a favorite of theoretical studies. Depending on the total energy, E_{tot}, collisions of protons with hydrogen molecules can have different outcomes, including rovibrational energy transfer, charge transfer, dissociation of the molecule into its atomic components, as well as radiative association leading to stable H_3^+. At energies below ~ 1.8 eV, proton exchange is the only reactive channel and we will limit our attention to this particular process. Early calculations starting in the 1970s[21–25] disclosed the main characteristics of the reaction dynamics. It was seen to evolve from a low energy behavior, dominated by capture into a strongly interacting complex, followed by a statistical breakdown of the three-atom complex, to the appearance of dynamical constraints with growing E_T, caused by increasingly direct collisions with shorter interaction times. These short interaction times do not allow for a complete randomization of the energy, angular momentum, and nuclear scrambling within the reaction intermediate. These calculations, based on simple statistical models, semiempirical potential energy surfaces (PESs) and a limited number of classical trajectories, could account reasonably well for the available experimental values of cross sections and rate coefficients,[9,26–30] which, on the other hand, present a certain scatter. Among the early theoretical approaches is the "most dynamically biased" (MDB) statistical model,[22] which used classical trajectories for defining complex formation and decay probabilities.[23] Using a set of only five parameters for all isotopic variants, this model could account for most experimental results ranging from thermal rate coefficients to state-to-state differential cross sections.[9,28]

Measurements on the H^+ + H_2 system were carried out mainly using deuterated isotopic variants, which are better suited for laboratory investigation, since they allow for a ready identification of reactants and products using methods of mass spectrometry. In addition to this practical advantage, the study of deuterated isotopologues of H^+ + H_2 is of interest for the gas-phase chemistry of the interstellar medium since some of these reactions are endoergic, due to the different zero-point energies (ZPE) of reactants and products, and can play an important role in the unusual deuterium fractionation observed in many cold space environments.[31–33] In fact, isotope selective effects due to deuterated variants of the H^+ + H_2 reaction are observable even in room temperature discharges of H_2/D_2 mixtures.[34]

Over the last two decades, great progress was achieved in the construction of accurate potential surfaces for the H_3^+ system[35–41] and in the development of gradually more rigorous theoretical approaches for the investigation of the nuclear motion. Refined statistical treatments, exhaustive quasiclassical trajectory (QCT) calculations, and time independent (TI) as well

as time dependent wave-packet (TDWP) quantum mechanical (QM) methods of varying accuracy were applied to the study of the H^+ + H_2 reaction dynamics (see for instance ref. 42–56 and references therein). Many of these theoretical works were centered on methodological aspects, emphasizing the comparison between different approaches. As a result of these studies it became clear that despite the apparent simplicity of the reaction considered all theoretical methods met with problems for the description of its dynamics. The validity of unbiased statistical models was found to be limited to slow collisions, methods based on classical mechanics were plagued by difficulties close to the reaction threshold, and precise QM calculations became awkward and computationally very expensive with growing collision energy due to the proliferation of bound states within the deep (~ 4.5 eV) potential well of the H_3^+ complex. In part due to these problems, a detailed comparison with existing experimental data was not attempted in most of the theoretical works just mentioned. An exception to this general trend is the recent article by Carmona-Novillo et al.[47] in which kinetic energy spectra, KES, from collisions of Rydberg H atoms, H*, with D_2 molecules at $E_T = 0.53$ eV were simulated with the results of H^+ + D_2 calculations. The dynamical similarity between the two systems had been recently discussed by Wrede et al.[57] and by Yang and co-workers.[58,59] In principle, KES, which include information both on the scattering angle and on the internal state distributions of the products, provide a stringent test of the accuracy of the PES and of the dynamical calculations complementary to the absolute values of total cross sections or rate constants. The simulation of the KES measurements from the Rydberg atom experiment showed just qualitative agreement between theory and experiment and exposed the discrepancies between the various theoretical approaches.[47] However, caution should be exercised when testing theoretical methods performed for ionic systems with the measurements carried out in collisions with Rydberg atoms.

In view of the situation described in the previous paragraph, a thorough comparison between theory and experiment that would allow a sound assessment of our present knowledge on the dynamics of this fundamental reaction seems timely. In the present work we attempt to make this assessment. To this end we have used the results from QCT, statistical QCT (SQCT), and QM calculations for the D^+ + H_2 and H^+ + D_2 reactions for the simulation of a comprehensive set of results from different experimental sources. The paper is organized as follows. In Section II, the theoretical methods are summarized. Section III provides some information on the various techniques and experiments used for measuring integral and differential cross sections or for getting thermal rate coefficients. Also the methods to account for the experimental averaging are mentioned. The detailed comparison of theory and experiment for D^+ + H_2 and H^+ + D_2 and the discussion of the results are presented in Section IV. The first reaction is exoergic, $\Delta H_0^\circ = -39.2$ meV, whereas the second one is endoergic with $\Delta H_0^\circ = 46$ meV (including the difference of ionization energies of the H and D atoms). The ensuing contrast in their threshold behavior is addressed in detail. In addition we have performed a theoretical simulation of kinetic energy spectra for the H^+ + D_2 system[60] over a significant range of E_T stretching from 0.40 eV to 2 eV.

This journal is © the Owner Societies 2012

Phys. Chem. Chem. Phys., 2012, **14**, 3346–3359 | 3347

II. Theoretical methods

A. Quantum mechanical method

For the $D^+ + H_2$ reaction time independent QM calculations have been carried out using the close-coupled hyperspherical method of Skouteris et al.[61] on the PES reported by Aguado et al.[36] The specific details of these calculations have been given in ref. 55. Suffice it to say here that the results have been obtained for a grid of 382 total energies in the range of 0.275 eV to 0.460 eV and initial rotational states $j = 0$–3. For $j = 0$ the reaction cross sections span the 5–190 meV relative translational energy range that are the same as those presented in a previous work.[55] The total cumulative reaction probability for $D^+ + H_2$ and that of its reverse $H^+ + HD$ reaction was used to calculate the respective thermal rate coefficients, $k(T)$.

The results for the $H^+ + D_2$ ($v = 0$, $j = 0$) reaction were obtained using a time dependent wave packet approach with the DIFFREAL-WAVE (DRW) code[62,63] on the PES by Kamisaka et al.[37] in a dense grid of E_T covering the 0.02–1.30 eV range. The calculations are however restricted to a maximum total angular momentum quantum number $J = 50$. This implies that fully converged results are only available for $E_T \leq 0.6$ eV. The details of these calculations have been presented in ref. 54. As shown in a previous work,[50] the differences between the QM results on the PES by Aguado et al. and by Kamisaka et al. are very minor for translational energies above 0.2 eV and largely irrelevant for the data presented and discussed here.

B. Statistical quasi-classical trajectory method

The statistical quasi-classical trajectory method (SQCT) has been described previously.[45,46,55] This model is, in all aspects, equivalent to its quantum mechanical version[64] with the only difference that in the SQCT model we run trajectories instead of propagating wave functions. The trajectories are integrated until the capture takes place which is assumed to occur when the potential takes a negative value ≤ -0.6 eV with respect to the corresponding asymptote.

In order to compare with the experimental kinetic energy spectra for the $H^+ + D_2$ reaction, batches of 5×10^5 trajectories were run at 0.4 eV, 0.524 eV, 0.6 eV, 0.8 eV and 2 eV (for the latter 1.5×10^6 trajectories were run) on the Aguado et al. PES.[36] Previous calculations with this methodology[54] using the PES by Kamisaka et al. at some of these energies lead to almost identical results. For the present calculations the initial and final atom–diatom distance was 12 Å and the time step was set to 1×10^{-16} s, enough to ensure a total energy conservation better than one in 10^5. Additionally, in order to determine specific rate coefficients and thermal rate constants for the $H^+ + D_2$ and $D^+ + H_2$ reaction, batches of 5×10^5 trajectories for other 41 energies in the energy range 1.0^{-3}–1.6 eV[55] were calculated. As the SQCT method complies with the reversibility principle, the data for the $H^+ + HD$ reaction did not require a separate calculation.

C. Quasi-classical trajectory method

Quasi-classical trajectory calculations have been performed for the $H^+ + D_2$ ($v = 0$, $j = 0$) reaction at the relative translational energies of 0.40 eV, 0.524 eV, 0.60 eV, 0.80 eV

and 2.0 eV on the PES by Aguado et al. by running batches of 1.5×10^6 trajectories at each energy. In addition, to test the influence of the D_2 rotation on the reactivity, calculations at 0.40 eV were carried out for initial $j = 1$. A large number of trajectories at each energy are required for the need to converge the state-to-state differential cross sections (DCS) to simulate the experimental results (see below).

The initial and final atom–diatom distance was set to 12 Å, and the integration step size used was 5×10^{-17} s, enough to guarantee a total energy conservation better than one part in 10^4. The rovibrational energies and the assignment of final sates were carried out as in previous works. In all cases the usual histogram binning (hereinafter HB) as well as the Gaussian binning (GB) (see ref. 54 and 55 and references therein) were used to determine the population in the final states. The latter procedure is especially convenient to avoid the violation of the zero point energy and the assignment of quantum numbers of states that are energetically closed. Its application to the calculations for the title reactions has been discussed at length in ref. 54 and 55. In this work the FWHM of the Gaussian weight function was set to 0.03 in order to describe correctly the energy threshold for the $H^+ + D_2$ reaction. Notice that in previous works[52,54] a FWHM of 0.1 was used for the GB weighting. As a result, the low temperature rate coefficients were higher.

The specific rate coefficients, $k(v_r) = \sigma_R(E_T)v_r$, where v_r is the relative velocity for $H^+ + D_2$ and $D^+ + H_2$ reactions were calculated using the excitation functions presented in ref. 55. Batches of 2×10^6 were run in the 0.24–1.20 eV total energy range to calculate the QCT cumulative reaction probabilities following the method described in ref. 65. The thermal averaged rate coefficients were determined for the abovementioned reactions and for $H^+ + HD \rightarrow D^+ + H_2$ following the procedure described in the Appendix of ref. 65. To this purpose, batches of 2×10^6 trajectories were run for each reaction in the 3×10^{-3}–1 eV collision energy range. For the $D^+ + H_2$ reaction additional batches of trajectories were run in the low collision energy range. Similar calculations were performed for the $H^+ + HD$ reaction, since the QCT method does not guarantee the compliance with the microscopy reversibility principle for the ensemble of trajectories.

III. Experiment and simulation

A. Experimental methods

In the following we summarize briefly those experimental results which have been obtained for low energy proton–proton or proton–deuteron exchange reactions in $H^+ + H_2$ collisions and isotopic variants. Although the H_3^+ ion in its stable form has been attracting more and more scientists in recent years, it is hard to believe that the most recent experimental studies of reactive collisions in this fundamental system are more than 20 years old. This means that all techniques here mentioned have already been summarized in reviews devoted to gas phase ion chemistry,[66] techniques for the study of ion–molecule reactions,[67] or state-selected and state-to-state ion–molecule reaction dynamics.[68] Additional details can be found in ref. 9, 32 and 69. Results include integral cross sections, rate coefficients under thermal and non-equilibrium conditions, and state to state differential cross sections.

1. Guided ion beams and merged beams. The first reliable absolute cross sections for $H^+ + D_2 \rightarrow D^+ + HD$ were reported by Ochs and Teloy,[26] older measurements are mentioned in this paper. These data were recorded with the first version of a guided ion beam (GIB) apparatus.[1] This instrument, which is in principle a tandem mass spectrometer, uses inhomogeneous oscillatory electric fields for guiding primary ions through a scattering cell. The technique provides a high detection efficiency for all primary and product ions, in the ideal case independent of mass, energy, and scattering angle. One of the most stringent tests is the conservation of total number of charges in the guide. Using a room temperature target gas, effective integral cross sections were determined as a function of the kinetic energy of the protons. The energy spread of the ions was close to 0.3 eV; the lowest translational energy reached was 0.3 eV. The error limit for the absolute value of the cross section was estimated to be 20%, mainly due to the uncertainty in determining the effective target density. In a newly developed, ultrahigh vacuum compatible GIB instrument, time-of-flight methods have been implemented for both selecting and calibrating the laboratory energy of the ions.[70] In this way, the accessible energy range could be extended down to nominal values as low as 25 meV. New results for H–D and D–H scrambling were measured in ref. 30. After these improvements, the limits for lowest energy and the energy resolution were given by the thermal motion of the target gas.

For a further extension of the GIB technique, the room temperature scattering cell had to be replaced by a supersonic beam. A real step forward was achieved by merging an intense supersonic beam and a slow ion beam guided within the neutral beam. For $D^+ + H_2$ a translational energy resolution as low as 7 meV has been achieved,[71] whereas for $H^+ + D_2$, the lowest attainable energy has been 20 meV, owing to the less favorable mass ratio $m_1 : m_2 = 1 : 4$. Using different expansion conditions, the rotational temperature of the hydrogen molecules can be controlled. The merged beam results cover an energy range of three orders of magnitude.

2. Swarms. A large body of kinetic and thermodynamic data were obtained using flowing afterglow (FA) and selected-ion flow tube (SIFT) techniques at room temperature. The variable-temperature selected-ion flow tube (VT-SIFT) opened up the range down to liquid nitrogen temperature (80 K). This method was used to determine rate coefficients at two temperatures.[28] These results seem to indicate a slightly different temperature trend. Temperatures down to a few K have been achieved by using instruments with cryogenic cooling or supersonic expansions; however, no results for the $H^+ + H_2$ system were obtained. To reach energies above room temperature, flow tubes are heated or the ions are accelerated in electrostatic fields (DRIFT).[29] Such an instrument has been used to study the H–D exchange. The rate constant values obtained tend to be smaller than those from other methods but mostly within the combined errors. One problem with H^+ or D^+ ions in He is to achieve steady-state average velocities at elevated electric field strengths (runaway effect), which limits the method to energies below ~ 0.3 eV.

3. Differential scattering. Beam methods can provide very detailed information on reaction dynamics; however, for a long time they have been restricted to higher energies, typically above 1 eV. Significant improvements in ion preparation, surface treatment, and the use of a radio frequency ion guides opened up the energy range down to 0.2 eV with high resolution. This specially designed differential scattering apparatus allowed us to determine velocity distributions for the D^+ products from the reaction $H^+ + D_2$.[60] In this experiment, the target gas was cooled down to liquid nitrogen temperature, the ion energy spread was 50 meV, and the angular resolution was 3°, resulting in an overall energy resolution of 80 meV. Product velocity distributions were determined by time of flight using a 1 m long octopole as a flight tube. The recorded spectra were transformed into laboratory energy distributions. These distributions show a structure due to partially resolved rovibrational states of the HD product molecule.

4. Ion traps. Another strategy to obtain experimental results at very low energies or temperatures makes use of ion traps in combination with cryogenic cooling. First results for $D^+ + H_2$ have been obtained with a liquid nitrogen cooled ring electrode trap.[72] They compare well with the swarm results reported in ref. 28. Also rate coefficients with para-enriched H_2 have been measured.[9] By choosing a suitable combination of number density and interaction time, rates for radiative association of H^+ with H_2 have been obtained.[73] Nowadays, temperature variable radio frequency ion traps are used in combination with temperature variable neutral beams.[74] Such instruments enable one to get state specific rate coefficients, e.g., for $D^+ + H_2$ ($v = 0$, j); however, no results have been published so far for the $H^+ + D_2$ ($v = 0$, j) reaction discussed in this paper.

B. Simulation of experimental data with theoretical results

A sound comparison between experimental and theoretical results implies the simulation of the raw experimental data. In the present case this includes the calculation of so-called 'effective' cross sections accounting for the experimental conditions. A special case is the simulation of the ion kinetic energy spectra (KES) measured at several LAB scattering data.

Simulation of the LAB kinetic energy spectra of scattered D^+ is carried out by transforming in each case the theoretical QM, SQCT and QCT CM v', j' DCS into the LAB system and performing the convolution with the experimental distributions of the H^+ beam velocity and divergence, the thermal distribution of the 'static' D_2 gas velocities, the scattering volume, and the detector aperture in and out-of-plane. The methodology and equations are the same or analogous as those used in previous works[75–77] and for simplicity will not be repeated here. Suffice it to say that the convolution consists in a multiple integral which is performed using a Monte Carlo sampling of the reagent beam velocities, the spatial H^+ beam density within the scattering volume defined by the beam divergence as it crosses the scattering chamber containing the D_2 gas, and the geometry of the detector. The CM → LAB transformation and convolution is carried out for each HD(v', j') rovibrationally resolved DCSs. The experimental detection efficiency at low kinetic energies is also taken into account (see ref. 60). Although the spread of relative translational energy is relatively small (FWHM 10%–20%), special care was paid to the variation of the state resolved DCS with

the translational energy. In particular, a grid of TDWP rovibrationally state resolved DCSs consisting of 160 collision energies in the 0.2 eV to 1.0 eV interval was used for the simulation. The averaging over collision energies proved to be important when using the QM DCSs since the state resolved flux into the specific range of scattering angles sampled by the experiments can change significantly with the collision energy due to the underlying resonance structure. It should be noted, however, that the QM simulations have been carried out with the results obtained for $j = 0$ D_2 initial rotational state.

IV. Results and discussion

A. Specific rate coefficients

We will first discuss the specific rate coefficients, $k(v_r; v, j) = \sigma_R(E_T; v, j)v_r$, where $\sigma_R(E_T; v, j)$ is the total (summed over all final states) reactive cross section as a function of relative translational energy for specific v, j state of the reagents, and v_r is the relative velocity. In particular, Fig. 1 shows the specific rate coefficients for the $H^+ + D_2$ ($v = 0, j$) reaction calculated with the three theoretical approaches considered in this work. Accurate TDWP quantum mechanical calculations are limited to $j = 0$ and are clearly recognizable in the figure by the sharp oscillations, indicative of a resonance structure that has survived the summation over partial waves. For the QCT calculations the results of the two binning procedures, HB and GB (see Section II), are included. The energetic threshold of $\sim$46 meV, mainly due to the difference in the zero point energies of D_2 and HD, is clearly observable in the results for $j = 0$ (upper left panel). Only the QCT-HB method, which ignores the zero point energy effect and hence the thermochemical threshold, predicts reactivity below $E_T = 40$ meV. Above this energy, the SQCT rate

coefficients show a monotonic increase with E_T in contrast with those from the "dynamical" methods (QCT and QM), which display a maximum at about 0.3 eV. The maximum value of the QM $k(v_r; v = 0, j = 0)$ is larger by about 25% than that from QCT methods. Except for a gradual decrease in the threshold with growing j, a similar behavior is observed in the evolution of the rate coefficients for $j = 1$ and $j = 2$. For $j = 3$, the internal energy of the system is enough to make the ground rovibrational state of the HD molecule energetically accessible at any translational energy and the threshold disappears.

Fig. 2 displays the corresponding rate coefficients for the $D^+ + H_2$ reaction. This exoergic isotopic variant has no threshold. Below 0.3 eV the rate coefficients calculated with the different methods are similar in magnitude except for those of the GB procedure for $j = 0$, and to a lesser extent for $j = 1$, which are smaller than the rest due to the low weight attributed by the method to trajectories whose internal energies lie below the ZPE of the HD molecule (see ref. 54 and 55 for more details). The specific rate coefficients from the three theoretical methods grow weakly with increasing E_T for all the j levels considered ($j = 0$–3). The QM results, which in this case are restricted to E_T lower than 200 meV, show the characteristic resonance oscillations, which decrease in intensity and frequency with growing j. Beyond 0.3 eV, the rate coefficients exhibit a behavior similar to that observed for $H^+ + D_2$ ($v = 0, j$). The QCT $k(v_r; v, j)$ drops with energy, whereas that from the statistical calculation goes on growing.

Fig. 3 provides an overview of theoretical calculations and experimental measurements of rate coefficients for the $H^+ + D_2$ reaction. The calculations correspond to a thermal internal state distribution of D_2 at a rotational temperature, T_{rot}, of 300 K, since most of the experiments were carried out with room
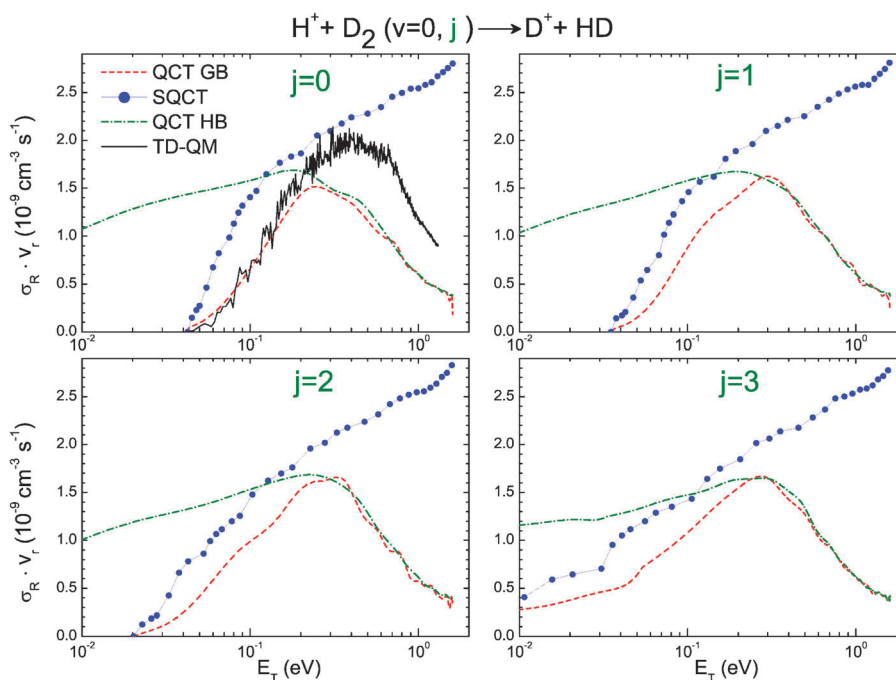

Fig. 1 Specific rate coefficient, $\sigma_R \times v_r$, for the $H^+ + D_2$ ($v = 0, j$) reaction for $j = 0, 1, 2,$ and 3 initial rotational states as a function of the relative translational energy, E_T, in logarithmic scale. Dot–dash (green) line: QCT-HB results. Dash (red) line: QCT-GB results. Solid (blue) line and solid circles: SQCT data. Solid (black) line wave packet QM results for $j = 0$.
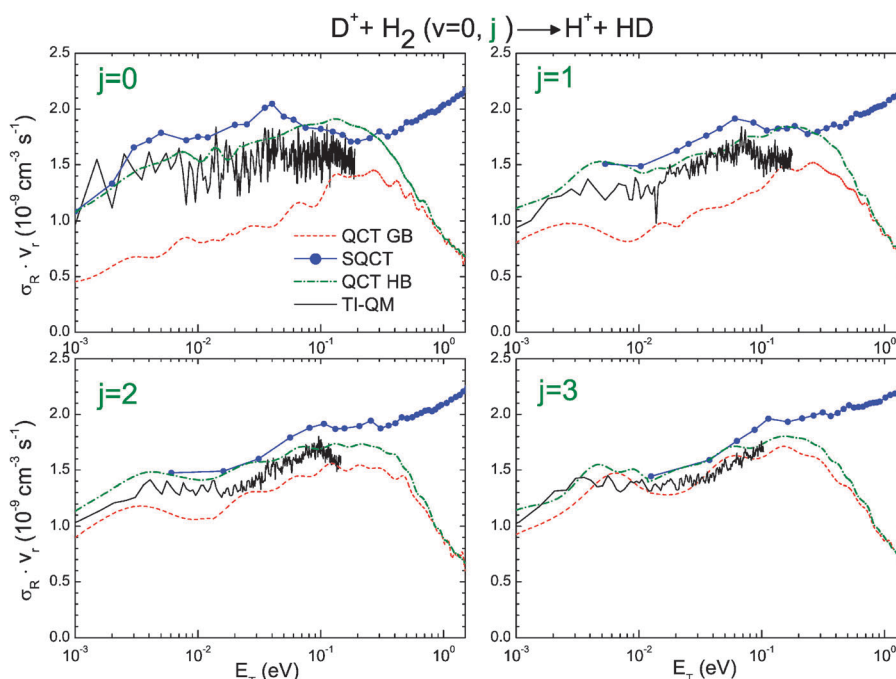
Fig. 2 Same as Fig. 1 but for the $D^+ + H_2$ $(v = 0, j)$ reaction, for $j = 0$–3. Here the solid (black) line represents the TIQM results.
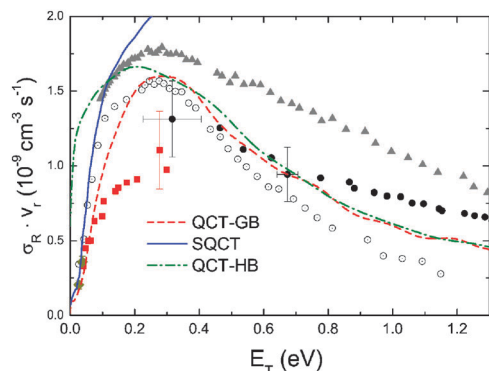

Fig. 3 Comparison of theoretical and experimental specific rate coefficients for $H^+ + D_2$ $(v = 0, \langle j \rangle) \rightarrow D^+ + HD$ vs. the relative translational energy. The theoretical results have been averaged over the thermal D_2 rotational state distribution (including the nuclear spin weights) at $T_{rot} = 300$ K. Dot–dash (green) line: QCT-HB results. Dash (red) line: QCT-GB results. Solid (blue) line: SQCT data. The experimental results are as follows: ⊙ Merged Beam (MB) results from ref. 9; solid (red) squares, DRIFT data from ref. 29; solid (black) circles, guided ion beam (GIB) measurements from ref. 26; solid (grey) triangles, GIB results from ref. 30; solid (dark yellow) rhombi selected-ion flow tube (SIFT) data from ref. 28.

temperature deuterium molecules. In spite of the appreciable data dispersion, a qualitative trend with an initial rise, a maximum, and a comparatively smooth post-maximum decline can be recognized as a general behavior. Only the statistical method, which ignores the dynamical restrictions to the reactivity—under the assumption that the collision complex is formed as long as the centrifugal barrier is overcome—fails to reproduce the presence of the maximum and grows monotonically. The best overall agreement is found between the merged beam (MB) experiments[9,71] and the QCT-GB calculations; in particular,

the experimental and theoretical values of the rate coefficient at the maximum are almost coincident. In the post-maximum decline the GB and HB QCT calculations are nearly indistinguishable and lie between the MB results and the guided ion beam, GIB, measurements of Ochs and Telloy.[26] The agreement is good taking into account the experimental uncertainty of typically 20%. The GIB measurements of Müller[30] cover the maximum and post-maximum energy range and yield systematically larger rate coefficients than those derived from the other experiments or from the dynamical QCT calculations; the discrepancies are smaller in the vicinity of the maximum. The lowest experimental values correspond to the drift tube experiments of Villinger et al.[29] which deviate significantly from the rest of the rate coefficients in the E_T interval between 0.1 eV and 0.3 eV. QM calculations have not been included in the comparison because they are not available for all the rotational states of D_2 needed for the thermal averaging at $T_{rot} = 300$ K. Based on the results for $j = 0$ (see Fig. 1), a very good agreement with the QCT-GB results is expected at $E_T < 0.2$ eV. However, at higher translational energies, the QM calculations for $j = 0$ yield appreciably higher rate coefficients than those from QCT and from the thermal experiments, with a value at the maximum close to 2×10^{-9} cm^3 s^{-1}. Recent QM results for $j = 1$[50] and the analogy with the classical results seem to indicate that the value of the rate coefficient at the maximum does not depend markedly on j and suggest that the discrepancy should persist in the thermally averaged QM calculations.

The lower energy interval before the maximum in the rate coefficient curves deserves a more careful consideration since threshold effects might be relevant for the results. Fig. 4 shows an enlargement for translational energies lower than 0.20 eV. In the upper panel of this figure, both the calculations and the experiments correspond to D_2 molecules with $T_{rot} = 300$ K.
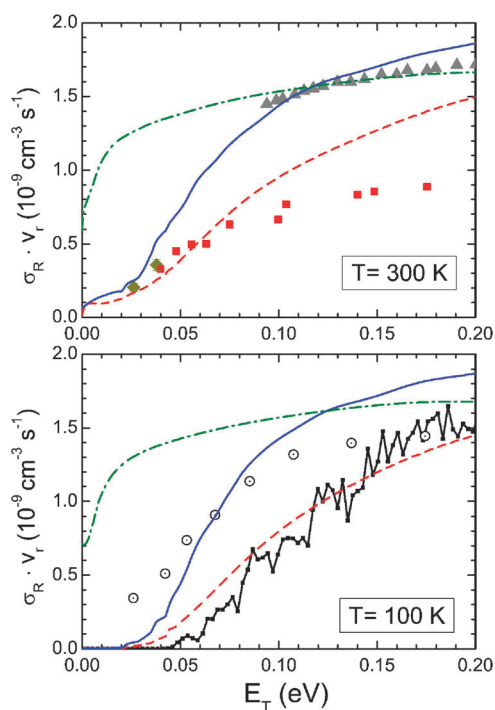
Fig. 4 Same as Fig. 3 but showing a more detailed comparison in the low energy range (up to 0.20 eV). The experimental and theoretical effective rate coefficients correspond to D_2 rotational distributions at $T_{rot} = 300$ K (upper panel) and $T_{rot} = 100$ K (bottom panel). For comparison purposes, the bottom panel includes the TDWP QM results calculated for $j = 0$ (solid black line with small squares).

The MB measurements[9] are represented in the lower panel. In these experiments the deuterium molecules have been supersonically expanded and are thus rotationally cold although without *ortho–para* relaxation. In order to mimic more closely the experimental conditions the rate coefficients for comparison with these data have also been calculated for $T_{rot} = 100$ K. The QM values for $j = 0$ (see Fig. 1) have been also represented in this panel. Although these results are not strictly thermal, the ground rotational level is the most populated state of D_2 at 100 K, and the comparison is meaningful. It is worth noting that for $T_{rot} = 300$ K, all the theoretical curves show some reactivity down to $E_T = 0$. The QCT-HB procedure yields always too large cross sections as compared with the QCT-GB results at the lowest translational energies for reactions with threshold. As discussed elsewhere,[54,55] the HB procedure, which does not take into account the zero point energy of the products, is not reliable under these circumstances and we will not consider it further in spite of the apparently good agreement with the GIB measurements (solid triangles).[30] The much smaller, but still visible, reactivity obtained with the QCT-GB and SQCT methods at $E_T = 0$ is due to the contribution of rotational states with $j = 3$ or larger (see Fig. 1), which begins to be appreciable for this temperature. In the E_T range between 0.10 eV and 0.20 eV, the GIB measurements of Müller[30] give larger values than those from the QCT-GB calculations, but are in good agreement with the results of the SQCT approach (remember, however, that the SQCT results diverge largely from the measurements at higher energies, as discussed in the previous paragraph).

The drift tube rate coefficients of Villinger *et al.*[29] (solid squares) lie below the calculated values over most of the energy range. Only at translational energies below 70 meV these measurements as well as those from flow tube (SIFT) experiments of ref. 28 are in good agreement with the SQCT and QCT calculations. For $T_{rot} = 100$ K, the QM, QCT-GB and SQCT rate coefficients are virtually zero for $E_T < 30$ meV and reflect more clearly the presence of the ground state reaction threshold. The QM and GB-QCT rate coefficients present a very similar post-threshold rise, which is slower than that from the SQCT calculations. The MB experimental values are in good agreement with the QM and QCT-GB result for $E_T > 0.15$ eV, but with decreasing energy they become larger and even surpass the SQCT rate coefficients. Note that in spite of the low T_{rot} of the D_2 molecules in the supersonic molecular beam of the MB experiment,[9] the MB rate coefficients in the vicinity of the threshold are curiously best reproduced with the SQCT results represented in the upper panel calculated for a D_2 rotational distribution at room temperature.

The upper panel of Fig. 5 displays the calculated and measured rate coefficients for the exoergic $D^+ + H_2$ deuteron exchange reaction covering the relative translational energy range from 0 to 1.2 eV, where measurements are available. The lower panel is an enlargement of the congested part of
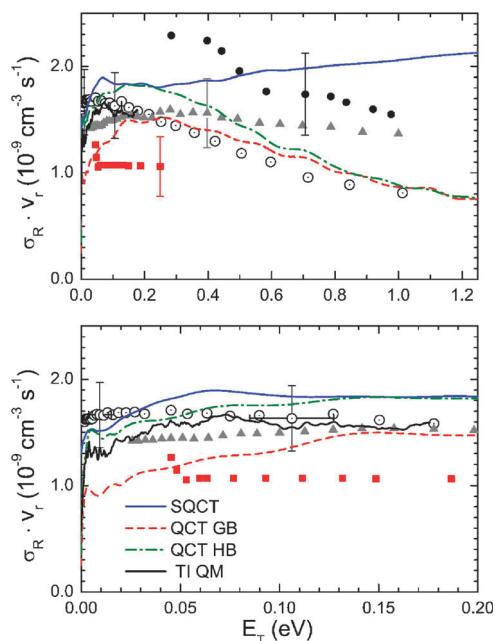

Fig. 5 Top: comparison of theoretical and experimental effective rate coefficients for $D^+ + H_2 (v = 0, \langle j \rangle) \to H^+ + HD$ in the 0.0–1.2 eV centre-of-mass translational energy range. The theoretical results have been averaged over the thermal H_2 rotational state distribution (including the nuclear spin weights) at $T_{rot} = 300$ K. Dot–dash (green) line: QCT-HB results. Dash (red) line: QCT-GB results. Solid (blue) line: SQCT data. Solid (black) line in the 0.0–0.18 eV range: TI QM results. The experimental results are as follows: ⊙ Merged Beam results from ref. 9; solid (red) squares, DRIFT data from ref. 29; solid (black) circles, guided ion beam (GIB) measurements from ref. 78; solid (grey) triangles, GIB results from ref. 30. Bottom: enlargement of the upper figure covering the low energy range of data, where the comparison with the TI QM results can be appreciated more clearly.

the figure below 0.2 eV. In this case all calculations correspond to T_{rot} = 300 K. Calculations performed with colder rotational distributions did not show an appreciable difference, as might be expected for a reaction without threshold. A considerable data dispersion exists also for this isotopic variant, but allowance must again be made for the large experimental uncertainty. Above E_T = 0.20 eV only the MB measurements and the QCT-GB calculations are in a good agreement. They both show a relatively slow decline of the rate coefficient with growing relative translational energy, similar to the one mentioned above for H^+ + D_2, but somewhat smoother. The rest of experimental and theoretical results are rather in disaccord with each other. The SQCT rate coefficients are too large in this energy range and keep on growing up to 1.2 eV, in contrast with the other calculations and measurements. As mentioned above and discussed elsewhere,[54,55] the unbiased statistical models are only adequate for slow collisions. The GIB experiments by Beyer[78] (solid circles) give the right descending trend with growing E_T, but the absolute $k(v_r)$ values are too high, comparable to those from the SQCT method. The GIB experiments of Müller[30] (solid triangles) and the QCT-HB results yield larger values than those from the QCT-GB calculations and from the MB experiments, but they lie mostly within the experimental uncertainty. As in the case of the H^+ + D_2 reaction, the two QCT methods lead to the same results beyond $E_T \approx 0.70$ eV. At this comparatively high energy the influence of the binning procedure in the total reaction cross section is negligible. In the low E_T range, below 0.20 eV (lower panel of Fig. 5), the effects of the binning method become already appreciable and, as commented on in the discussion of Fig. 2, the QCT-GB method tends to under-estimate the values of the rate coefficients. In this energy interval only the drift tube experiments of Villinger et al.[29] yield lower $\sigma_R v_r$ values than the rest of experiments and calculations. The best agreement is found between the MB measurements and the QM calculations, but also the QCT-HB results, and the SQCT calculations lie within the experimental uncertainty.

B. Thermal rate coefficients

The comparison of experimental and theoretical thermal rate coefficients, $k(T) = \langle \sigma_R(E_T) v_r \rangle_T$, is shown in Fig. 6. The experimental $k(T)$ were derived either from measurements using the flowing afterglow (FA)[27] or from selected ion flow tube (SIFT)[28] techniques. In contrast with the ion-beam measurements commented on thus far, where the relative translational energy was specifically selected independently of the internal states' distribution of the molecules, the results portrayed in Fig. 6 correspond to thermal equilibrium among the various degrees of freedom of the reactants.

The average relative translational energies of the thermal experiments presented here are lower than 50 meV and correspond thus to the lowest energy range sampled in the previous ion beam experiments. The upper panel of Fig. 6 corresponds to the exoergic D^+ + H_2 isotopic variant. As expected for a barrierless ion–molecule reaction, all calculations lead to a weak temperature dependence of the rate coefficients. In addition, the results of the QCT-GB lie below those of the other theoretical approaches. The experimental point at 295 K is in very good agreement with
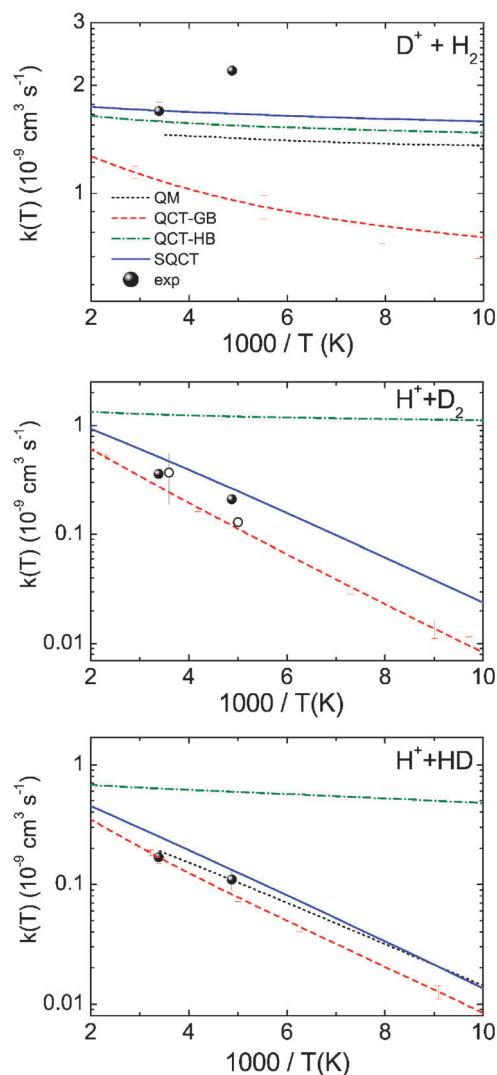

Fig. 6 Arrhenius plot of the thermal rate coefficients, $k(T)$, for the D^+ + H_2 (top panel), H^+ + D_2 (middle panel), and H^+ + HD → D^+ + H_2 (bottom panel) reactions, where the experimental results of ref. 28 (solid circles) and from ref. 27 (open circles) are compared with the theoretical results: QCT-HB results (dot–dash green line), QCT-GB results (dash red line), and SQCT data (solid blue line), and TI QM results (dotted black line).

the SQCT value and not too far from that of the QCT-HB method, which performs well for integral cross sections in reactions without threshold. QM results, which are available for a slightly lower temperature, lead to a $k(T)$ smaller than the measured one by about ~15%. The experimental point at 205 K is too high and at variance with all the calculations, which suggests that the measurement may be flawed.

The two lower panels of Fig. 6 correspond to deuteron–proton exchange reactions (H^+ + D_2 and H^+ + HD) with an energetic threshold, and their rate coefficients increase with temperature exhibiting an approximate Arrhenius functionality. The QCT-HB method, which ignores the existence of the threshold, predicts a behavior similar to that found for D^+ + H_2, with a weak temperature dependence for $k(T)$, and fails thus to account for the measured rate coefficients. The existing experimental data[27,28] for the H^+ + D_2 reaction seem to be encompassed by the

SQCT and QCT-GB rate coefficients, slightly closer to the former. The low temperature QCT-GB rate coefficients for this reaction reported in previous work[52] were somewhat higher due to a difference in the choice of the Gaussian width (see Section IIC). The QM $k(T)$, which is available for the $H^+ + HD \rightarrow H_2 + D^+$ reaction, and the QCT-GB $k(T)$ are in reasonable agreement with the measurements for this reaction.[28] The SQCT rate coefficients are also in reasonable accordance with the measured rate constants, but tend to overestimate the higher T points, suggesting that the dynamical bias mentioned above is already appreciable at room temperature.

It should be noted at this point that the previously mentioned MDB model[22,23] using five parameters (which were determined using trajectory calculations and the criterion "number of minimum exchanges" for the definition of complex formation) could reproduce most of the merged beam data and thermal coefficients of Fig. 3–6 with semiempirical surfaces of the diatomics-in-molecules (DIM) type.[9,23,32]

C. Kinetic energy spectra

This last subsection is devoted to the comparison of the experimental and simulated laboratory (LAB) kinetic energy spectra (KES) of D^+ ions generated in $H^+ + D_2$ reactive collisions. The theoretical simulations have been carried out using the complete set of state-to-state differential cross sections calculated with the QCT, SQCT and QM data as it has been described in Section IIIB. These LAB KES are nothing but the measurement of the relative flux of the D^+ product scattered into a fixed LAB scattering angle as a function of the D^+ recoil energy in the LAB frame. As mentioned in Section IIIA3, the D_2 target gas is kept at ~ 80 K and consequently $j = 0$ is the most populated state.

In Fig. 7 the KES are depicted for a laboratory (LAB) angle $\Theta = 5°$ at three translational energies. This LAB angle corresponds roughly to centre-of-mass (CM) scattering angles in the 160°–180° interval with some contribution from forward scattering at low LAB kinetic energies—as customary, the CM scattering angles are defined as the angle between the scattered HD molecule and the incoming H^+. These spectra show a broad energy distribution with its maximum at high kinetic energies, and secondary maxima for lower D^+ kinetic energies. The large width of the KES indicates that much of the initial kinetic energy of the collision is redistributed within the HD_2^+ intermediate complex and then channeled into the internal energy of the products. For the two lower E_T (0.40 eV and 0.52 eV), represented in the two upper panels, the experimental spectra have been simulated using results from the three theoretical methods. Fully converged QM calculations extend to $E_T = 0.60$ eV, but they are not enough for a rigorous simulation of the experiments which requires data beyond those at 0.60 eV due to the translational energy spread, which is ~ 0.1 eV (FWHM) at this translational energy. Therefore a QM simulation is not included in the lower panel of Fig. 7 (however, see hereinafter for a more detailed consideration of the available QM data). Although most of the simulations have been carried out using the complete set of state-to-state DCS for the initial rotational state $j = 0$, simulations have also been performed adding the contribution from $j = 1$ calculated
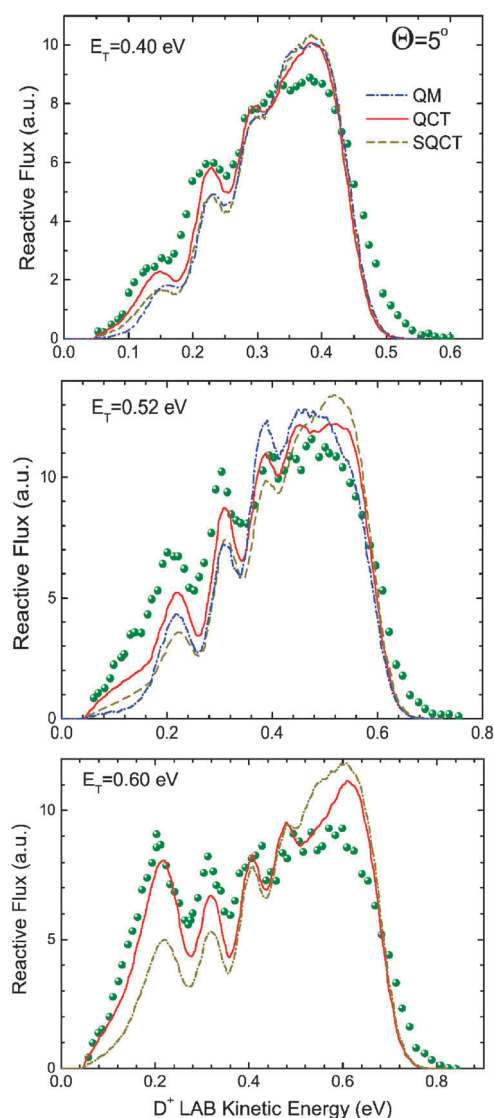

Fig. 7 LAB Kinetic Energy Spectra (LAB KES) of the D^+ ion at a laboratory angle $\Theta = 5°$ from the $H^+ + D_2 \rightarrow HD + D^+$ reaction at $E_T = 0.40$ eV (top panel), $E_T = 0.52$ eV (middle panel) and $E_T = 0.60$ eV (bottom panel). Experimental points (green) solid points; QCT-GB results solid (red) line; SQCT dashed (dark yellow) line; TDWP QM results dash-dot (blue) line.

using the QCT-GB and SQCT approaches. In any case, the inclusion of this rotational state in the QCT and SQCT simulations is practically negligible in the final shape of the KES. However, as mentioned in Section IIIB, the simulation requires the inclusion of the energy dependence of the state-to-state DCSs in the range of translational energies spanned by each experiment, which has been found to be well represented by a nearly Gaussian distribution with a FWHM of 10% to 20% of the mean translational energy in each case. Whereas for the simulations with SQCT and QCT results this effect proved to be very minor, in the case of the simulations with QM results the consideration of this dependence was found to be mandatory since the state-resolved CM DCSs for backward and forward scattering angles change very rapidly with the collision energy. In this respect, the availability of data with a very fine grid of translational energies resulting from the TDWP calculations was most useful.

The general patterns of the experimental KES in Fig. 7 are reasonably well reproduced by the calculations, but some discrepancies are also found. In all cases, the measured spectra are slightly broader and stretch toward somewhat higher energies than the calculated ones. The best overall agreement between theory and measurements is obtained with the QCT-GB results and the worst simulations correspond to the SQCT method; the QM calculations are somewhere in-between. The QCT-HB rotational distributions are not too different from those of QCT-GB at the comparatively high relative translational energies of these experiments[54] and the corresponding simulations have not been included in Fig. 7. In the following we will not consider the HB method, which, as discussed above, is less appropriate for reactions with a threshold, and will tacitly assume that all QCT results correspond to the GB procedure. The theoretical calculations allow also an identification of the internal states of the HD product molecule responsible for the main features of the measured spectra. This is exemplified in Fig. 8 for $\Theta = 5°$ and $E_T = 0.40$ eV; i.e., the conditions of the upper panel of Fig. 7. At this relative translational energy, virtually all HD molecules are generated

in the ground vibrational state, $v' = 0$. The simulations show that the big broad maximum to the right corresponds to an unresolved set of low rotational states ($j' = 0–5$) and the two descending maxima to the left are mostly associated with the $j' = 6$ and 7 levels. The QCT j' distribution, which peaks at $j' = 5$, is slightly warmer than its QM counterpart, that has a maximum at $j' = 4$; and it is precisely the larger relative contribution of the QCT higher rotational levels to the total distribution, what leads to a better agreement of the QCT KES with the measured data.

At higher energies, vibrationally excited states begin to play a role. For $E_T = 0.60$ eV (lower panel of Fig. 7), there is a noticeable rise of the lowest kinetic energy peak in the KES, due to the appearance of HD molecules in the $v' = 1$ level. The QCT results lead again to an overall good accordance with the measurements, with a slight overestimation of the high energy peak. The SQCT simulation is, in contrast, appreciably worse. For even higher E_T, the participation of vibrationally excited states of HD in the KES becomes much more important. Fig. 9 portrays the KES at three LAB scattering angles for $E_T = 0.80$ eV. As can be seen, the maxima have shifted to the low kinetic energy (high internal energy) end of the spectra, due to the significant contribution of the $v' = 1$ state to the global reactive scattering. At this E_T the QCT calculations can reproduce again the measured KES for the three scattering angles represented in Fig. 9. The SQCT method, however, leads to a partition of energy in the products with a larger fraction in translation and a smaller fraction in vibration and, especially, in rotation (see ref. 54 and Fig. 7 of ref. 55), and is unable to account for the higher degree of internal excitation produced in increasingly faster collisions and reflected in the kinetic energy spectra. The gradual failure of the SQCT method for the reproduction of the experimental KES with growing translational energy is not unexpected, since, as commented on elsewhere,[22,23,52] faster collisions lead to a defective randomization of energy in the complex and thus to a deviation from the statistical behaviour. Moreover, as it has been discussed elsewhere,[24,54] as the energy increases, the surmounting of the barrier does not necessarily imply the formation of long-lived complexes and, as a matter of fact, the incoming H^+ ion interacts very little with the D_2 molecule that remains essentially unperturbed. As a result, the collision is practically direct and no reaction takes place. The apparently better performance of QCT as compared to QM calculations hinted at in the simulated spectra for $E_T = 0.40$ and 0.52 eV (two upper panels of Fig. 7) deserves further consideration.

Fig. 10 shows the theoretical opacity functions, i.e., the reaction probabilities, $P(J)$, as a function of the total angular momentum, for the $H^+ + D_2$ reaction for $E_T = 0.60$ eV and 0.80 eV. The QM reaction probabilities, which are easily recognizable by their sharp oscillatory structure, are not converged beyond $E_T = 0.60$ eV since coupled channel calculations including all Coriolis couplings were only practically feasible up to $J = 50$. They are found to be smaller than those from the SQCT model, but larger than those from QCT for most J values. This trend was already observed and discussed more thoroughly for lower energies (see ref. 54). The largest divergence between the three methods is found for $J > 20$; below this value the QM and QCT results are in good agreement. Overall at $E_T = 0.60$ eV the QM results are closer to those from SQCT
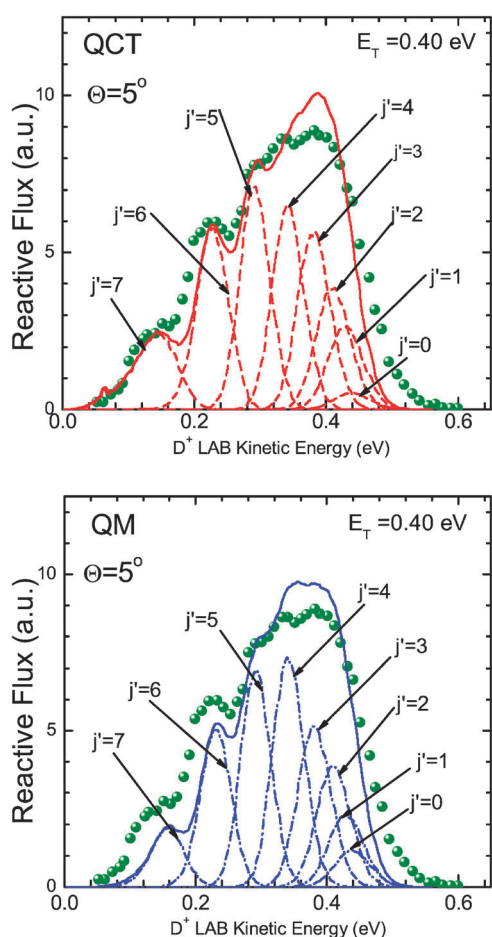

Fig. 8 Rotationally resolved LAB Kinetic Energy Spectra (LAB KES) of the D^+ ion at a LAB angle $\Theta = 5°$ from the $H^+ + D_2 \rightarrow HD + D^+$ reaction at $E_T = 0.40$ eV. This LAB angle corresponds approximately to 170°–180° CM angles (backward scattering) with some smaller contribution from 0° to 30° CM angles. Upper panel: QCT-GB results. Lower panel: TDWP QM results. Lines and points as in Fig. 7.
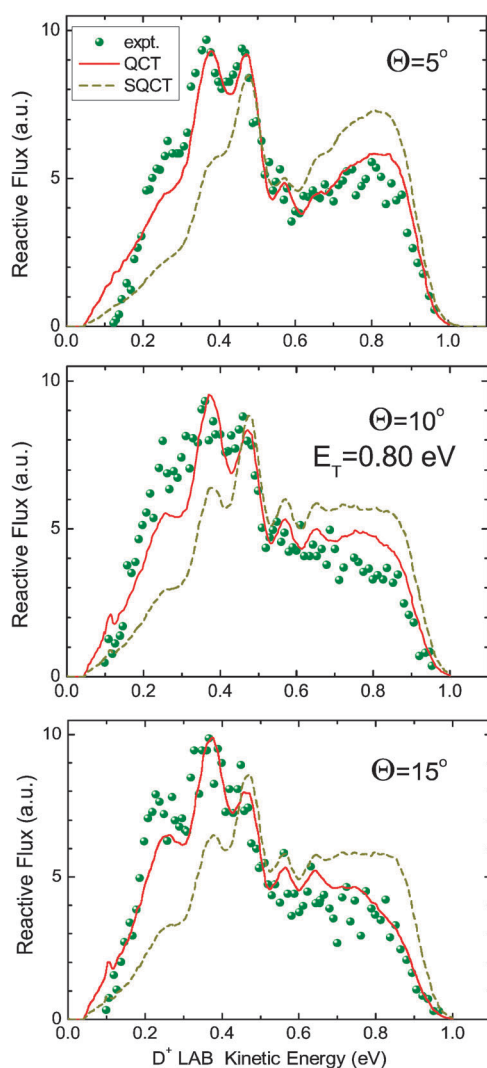
Fig. 9 D$^+$ ion KES at $\Theta = 5°$ (top panel), 10° (middle panel), and 15° (bottom panel) laboratory angles from the H$^+$ + D$_2$ → HD + D$^+$ reaction at $E_T = 0.80$ eV. This LAB angle corresponds approximately to CM backward scattering angles. Lines and points as in Fig. 7.

and at $E_T = 0.80$ eV are more equidistant between the QCT and SQCT opacity functions. Previous analyses[54,55] concluded that high J values (i.e., high impact parameters), $J > 40$, contribute only to reaction in low rovibrational states. Since the QCT calculations predict a much smaller participation of these high-J values, it is expected, and indeed is what it occurs, that the resulting rovibrational distributions are considerably hotter than those resulting from SQCT and, to a lesser extent, from QM calculations.

The discrepancy between the QM and QCT opacity functions just commented on is intriguing, especially considering the good agreement between the experimental KES and the QCT simulations for these two energies (Fig. 7 and 9). Although, the QM results are expected to be more accurate, the similitude in magnitude of the opacity functions from QM and SQCT suggests that the existing QM results might also disagree with the observed kinetic energy spectra. A possible way out of this dilemma would be a hypothetical selectivity of the experiment to the lower J values ($J < 20$), where the QCT and QM
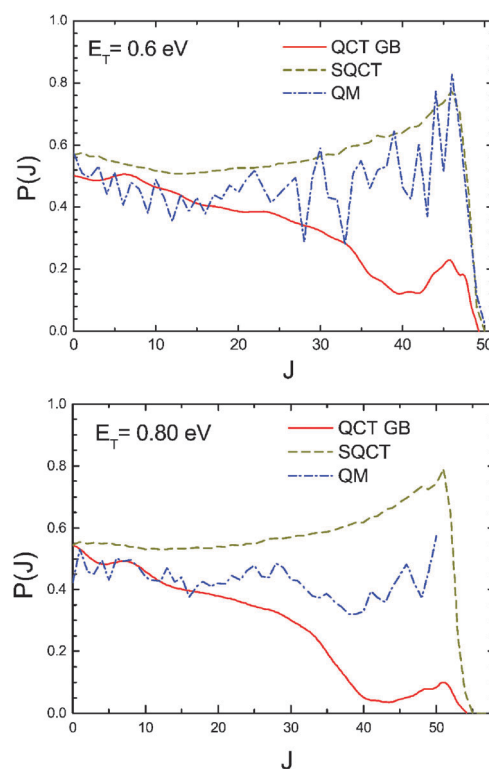

Fig. 10 Total reaction probability, $P(J)$, as a function of total angular momentum, J, for the H$^+$ + D$_2$ ($v = 0$, $j = 0$) reaction at $E_T = 0.60$ eV (upper panel) and $E_T = 0.80$ eV (lower panel). QCT-GB results solid (red) line; SQCT dashed (dark yellow) line; TDWP QM results dash-dot (blue) line.

probabilities are in rough accordance and differ somewhat from the SQCT calculations. This could be the case if the DCS at backward angles, as those mainly sampled by the experiment, would be predominantly made up by low J values. In order to check this possibility, QM and QCT simulations of the KES were performed alternatively with DCSs calculated including either $J < 25$ or all available J values. Note that the QM calculations extend only until $J = 50$. This includes virtually all J necessary for convergence at $E_T = 0.60$ eV (see the opacity function of Fig. 10 at this energy), but falls somewhat short for $E_T = 0.80$ eV. In any case, an inspection of Fig. 10 suggests that even for the latter energy, most of the relevant angular momenta are included in the QM calculations. Thus, although the QM simulations are not completely rigorous, we believe them to be meaningful for the present discussion. The results of the QM and QCT simulations are represented in Fig. 11 together with the corresponding experimental data. For comparison, the more complete calculations, extending to the largest J available in each case, have been scaled to the measured points. The simulations with the DCSs calculated with $J_{max} \leq 25$ have used in each case the same scaling factor, such that these results represent the contribution to the total KES from the low range of J values. An inspection of Fig. 10 shows immediately that the experiments sample all the available Js or, in other words, that the CM DCSs at those angles mainly sampled by the experiment contain contributions from the whole range of J-partial waves. It is also clear that the QCT results lead to a surprisingly better agreement with the measurements
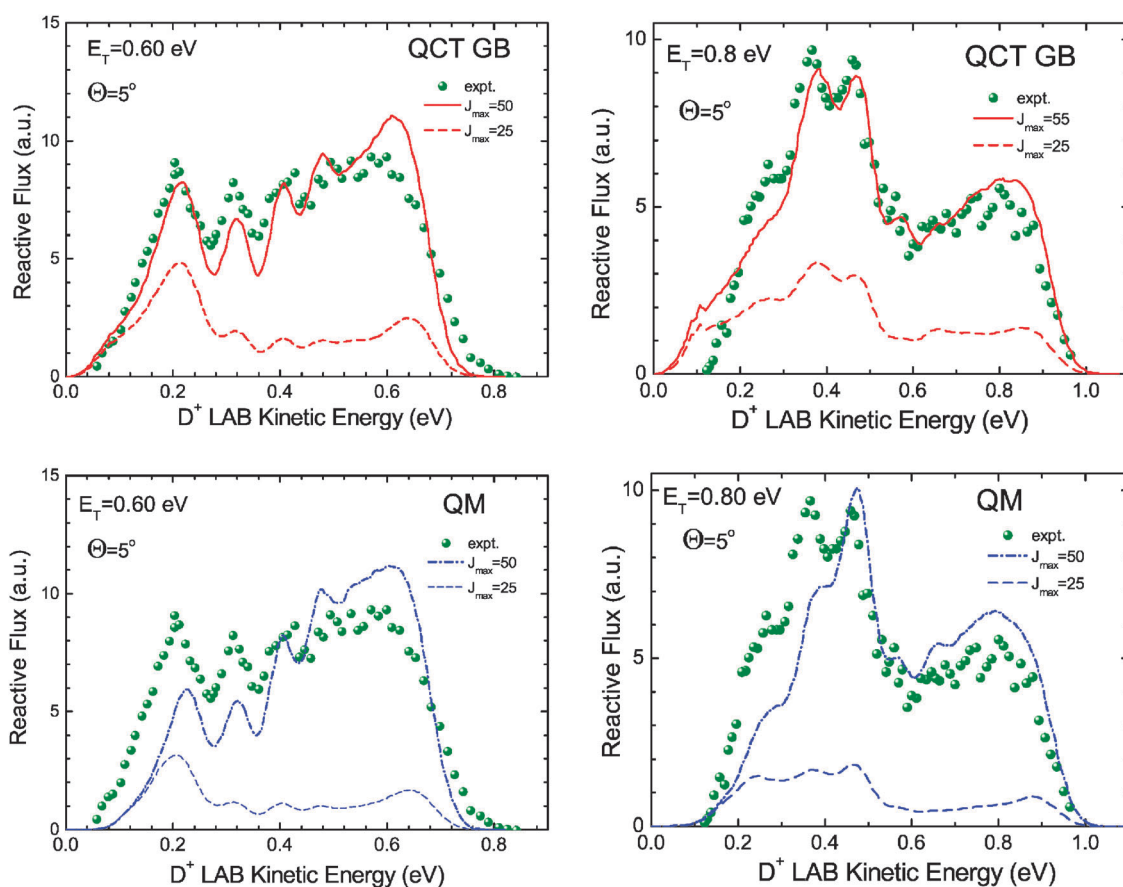
Fig. 11 Experimental and simulated D^+ ion LAB KES for the $H^+ + D_2 \rightarrow HD + D^+$ reaction at a LAB angle of $\Theta = 5°$ at the indicated relative translational energies. Green solid points represent the experimental data. Upper left panel: QCT-GB results at $E_T = 0.60$ eV. Solid (red) line calculations for $J_{max} = 50$; dashed (red) line, contribution from $J \leq 25$. Upper right panel: same for $E_T = 0.80$ eV. Lower left panel: TDWP QM calculations at $E_T = 0.60$ eV. Dash dot (blue) line, calculations including all angular momenta up to a maximum value $J_{max} = 50$; dashed (blue) line, contribution from $J \leq 25$. Lower right panel: same for $E_T = 0.80$ eV. Note that partial waves beyond $J = 50$ are necessary for an accurate simulation with the QM results. See text for details.

than those from the QM calculations. For $E_T = 0.60$ eV, collisions with $J < 25$, corresponding to low impact parameters, lead to a more efficient production of rovibrationally excited HD molecules, as shown by the dominance of the peak at $E_{LAB}(D^+) = 0.20$ eV which is associated to $v' = 1$. In contrast, collisions with higher J values populate preferentially low rotational levels of HD as demonstrated by the pronounced rise of the broad maximum toward the high energy end of the distribution upon inclusion of all angular momenta up to $J = 50$. The immediate conclusion is that the difference between the simulations carried out with QM and QCT lies in the respective relative contribution from high J values, whereas the QM and QCT contributions from $J < 25$ are very similar. For $E_T = 0.80$ eV more states come into play and the just mentioned correlations are not so evident in the spectra. Notwithstanding, it is clear that at this energy the QM simulation suffers from the lack of a more significant participation of the most excited states of the HD product. Even if these calculations were carried out with all the necessary partial waves for convergence ($J_{max} \approx 55$), one can reasonably expect very little contribution from the high J values to the low energy part of the KES given the low propensity of those partial waves to produce internally excited products.

Finally, the good performance of the QCT method and the failure of the SQCT approach at high energies are particularly evident in Fig. 12, where the kinetic energy spectrum for $E_T = 2.0$ eV at $\Theta = 5°$ is represented. At this energy QM calculations are too far from convergence to be considered even approximately. At this translational energy some participation of non-adiabatic processes can be expected with the opening of charge transfer channels and the consequent decrease of the reactive adiabatic channel. However, the existing calculations[37,79,80] show that this effect is not so important and it would unlikely affect the relative contributions of the various rovibrational states to the DCS. As can be appreciated, the maxima in the spectrum simulated with the SQCT data are clearly shifted toward higher D^+ kinetic energies as compared to those in the measured one, thus failing to reproduce the observed spectrum. Once more, the QCT calculations, which incorporate naturally the dynamical bias of more direct collisions, can simulate the measurements satisfactorily. An analysis of the QCT results allows the identification of the HD vibrational states contributing to the distinct peaks in the structure of the KES. The result of this analysis in terms of the cumulative contributions from the successive vibrational states is shown in the lower panel of Fig. 12.
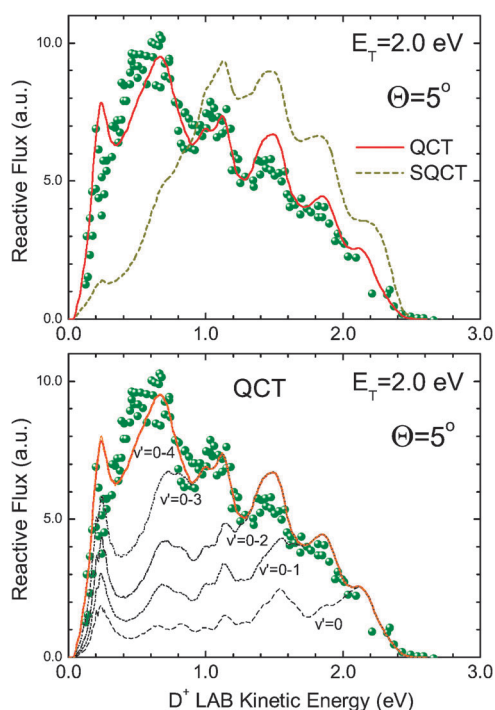
Fig. 12 D^+ ion KES at a laboratory angle $\Theta = 5°$ from the $H^+ + D_2 \rightarrow HD + D^+$ reaction at $E_T = 2.0$ eV. Top panel: comparison of experimental (solid green points), QCT-GB (solid red line) and SQCT (dotted dark yellow line) results. Bottom panel: cumulative vibrationally resolved spectra (see text for details).

It should be borne in mind that no information about the absolute value of the cross section is contained in the KES discussed in this section. Only the relative contributions from the different states to the differential cross section is revealed.

V. Summary and conclusions

A detailed comparison of theoretical calculations with available experimental data on the dynamics of the $H^+ + D_2$ and $D^+ + H_2$ reactions has been carried out. The experimental data include state specific rate coefficients for selected E_T up to 1.2 eV, thermal rate constants at 300 and 200 K, and, in the case of $H^+ + D_2$, kinetic energy spectra of the D^+ ions generated in the reaction for E_T between 0.4 and 2 eV. The calculations have been performed on accurate *ab initio* potential energy surfaces using three theoretical approaches, QM, QCT, and SQCT. Special care has been given to the precise simulation of the experimental conditions. The QM calculations have been done either with a time dependent wave packet (TDWP) method ($H^+ + D_2$) or with a time independent formalism ($D^+ + H_2$), and are limited to a lower range of E_T and internal states than the other two approaches. In the QCT method, two binning procedures have been used for the assignment of quantum states, the conventional histogram binning (HB) and a Gaussian binning (GB), giving more weight to trajectories with vibrational actions close to the actual quantum values of the products.

Rather surprisingly, the QCT-GB method leads to the best overall agreement between experiment and theory for the two reactions, over the broad range of relative translational energies investigated. In particular, it can reproduce satisfactorily

the kinetic energy spectra measured for the $H^+ + D_2$ reaction for E_T between 0.4 eV and 2.0 eV. However the method gives too low cross sections for the barrierless $D^+ + H_2$ reaction at the lower energies investigated, including those relevant for the room temperature rate constant which is underestimated by $\sim 50\%$. The QM treatments perform also well for the calculation of cross sections and rate coefficients in the limited range of E_T where they are available. The TDWP calculations for $H^+ + D_2$ seem to overestimate the specific rate coefficients in the 0.2–0.6 eV range. However, an accurate comparison with the experimental specific rate coefficients averaged over a rotational distribution at a given temperature would require to extend the WP calculations to initial rotational states other than $j = 0$. TDWP QM results account also reasonably well, albeit somewhat worse than QCT-GB, for the KES at 0.40 eV and 0.52 eV, where rigorous simulations are possible. However, the available QM calculations, which in some cases are close to convergence, suggest that the simulated QM KES are likely to disagree with the measurements at higher energies. The SQCT model gives the worst global agreement. It is only adequate for low relative E_T. Beyond $E_T = 0.20$ eV it leads to exceedingly large rate coefficients. In addition, for relative translational energies larger than 0.60 eV it cannot account for the high internal excitation of the products revealed by the experimental KES. These discrepancies are consistent with the finding that the title reactions rapidly depart from a pure statistical behaviour as the translational energy increases beyond 0.5 eV.[52,54,55] Among the various experimental approaches for the determination of energy selected rate coefficients the merged beam (MB) method seems the most reliable. Its consistency with the QCT-GB results for the two reactions over the largest energy range suggests that the MB data might supersede the previous drift tube and guided beam measurements.

The most significant discrepancy between experiment and theory is found in the values of the rate coefficients of the $H^+ + D_2$ isotopic variant for $E_T < 0.2$ eV, where no theoretical calculation can satisfactorily reproduce the experimental data. Particularly puzzling is also the seeming inability of the present TDWP differential cross sections to account for the experimental kinetic energy spectra at $E_T > 0.5$ eV. Additional QM calculations on the most recent global PES available[40] spanning a larger range of translational energies and therefore comprising higher values of J, as well as including more initial rotational states are probably needed for a more rigorous simulation of the measurements.

In summary, the present results invite further experimental and theoretical investigations of the reaction dynamics of this deceptively simple reaction both at superthermal relative translational energies and at low energies nearby the reaction threshold, where it is relevant to astronomical environments.

3358 | *Phys. Chem. Chem. Phys.*, 2012, **14**, 3346–3359

This journal is © the Owner Societies 2012

References

1 E. Teloy and D. Gerlich, *Chem. Phys.*, 1974, **4**, 417.
2 N. G. Adams, *Int. J. Mass Spectrom. Ion Processes*, 1976, **21**, 349.
3 N. G. Adams and D. Smith, in *Reactions of small transient species*, ed. A. Fontijn and M. A. A. Clyne, Academic Press, London, 1983, p. 311.
4 H. Bohringer and F. Arnold, *Int. J. Mass Spectrom. Ion Processes*, 1983, **49**, 61.
5 R. B. Rowe and J. B. Marquette, *Int. J. Mass Spectrom. Ion Processes*, 1987, **80**, 239.
6 S. T. Graul and R. R. Squires, *Mass Spectrom. Rev.*, 1988, **7**, 263.
7 P. R. Kemper and M. T. Bowers, *J. Am. Soc. Mass Spectrom.*, 1990, **1**, 197.
8 M. Hawley, T. L. Mazely, L. K. Randeniya, R. S. Smith, X. K. Zeng and M. A. Smith, *Int. J. Mass Spectrom. Ion Processes*, 1990, **97**, 55.
9 D. Gerlich, *Adv. Chem. Phys.*, 1992, **82**, 1.
10 P. Tosi, *Chem. Rev.*, 1992, **92**, 1667.
11 D. Gerlich, *J. Chem. Soc., Faraday Trans.*, 1993, **89**, 2199.
12 D. Gerlich, *Phys. Scr.*, 1995, **T59**, 256.
13 M. A. Smith, *Int. Rev. Phys. Chem.*, 1998, **17**, 35.
14 I. W. M. Smith and R. B. Rowe, *Acc. Chem. Res.*, 2000, **33**, 261.
15 S. D. Smith, *Chem. Rev.*, 1992, **92**, 1473.
16 E. Herbst, *Chem. Soc. Rev.*, 2001, **30**, 168.
17 T. P. Snow and V. M. Bierbaum, *Annu. Rev. Anal. Chem.*, 2008, **1**, 229.
18 B. J. McCall, T. R. Geballe, K. H. Hinkle and T. Oka, *Astrophys. J.*, 1999, **552**, 338.
19 E. M. Hollmann and A. Y. Pigarov, *Phys. Plasmas*, 2002, **9**, 4330.
20 I. Méndez, F. J. Gordillo, V. J. Herrero and I. Tanarro, *J. Phys. Chem. A*, 2006, **110**, 6060.
21 J. R. Krenos, R. K. Preston, R. Wolfgang and J. C. Tully, *J. Chem. Phys.*, 1974, **60**, 1634.
22 D. Gerlich, U. Nowotny, C. Schlier and E. Teloy, *Chem. Phys.*, 1980, **47**, 245.
23 D. Gerlich, in *Symposium on Atomic and Surface Physics*, ed. W. Lindinger, F. Howorka, T. D. Märk and F. Egger, Institut fuer Atomphysik der Universitat Innsbruck, Innsbruck, 1982, p. 304.
24 C. Schlier and U. Vix, *Chem. Phys.*, 1987, **113**, 211.
25 M. Berblinger and C. Schlier, *J. Chem. Phys.*, 1994, **101**, 4750.
26 G. Ochs and E. Teloy, *J. Chem. Phys.*, 1974, **61**, 4930.
27 F. C. Fehsenfeld, D. L. Albritton, Y. A. Bush, P. G. Fournier, T. R. Govers and J. Fournier, *J. Chem. Phys.*, 1974, **61**, 2150.
28 M. J. Henchman, N. G. Adams and D. Smith, *J. Chem. Phys.*, 1981, **75**, 1201.
29 H. Villinger, M. J. Henchman and W. Lindinger, *J. Chem. Phys.*, 1982, **76**, 1590.
30 D. Müller, *Diploma thesis*, University of Freiburg, Germany, 1983.
31 W. D. Watson, *Astrophys. J.*, 1973, **181**, L129.
32 D. Gerlich and S. Schlemmer, *Planet. Space Sci.*, 2002, **50**, 1287.
33 T. J. Millar, *Astrophys. Geophys.*, 2005, **46**, 2.29.
34 M. Jiménez-Redondo, E. Carrasco, V. J. Herrero and I. Tanarro, *Phys. Chem. Chem. Phys.*, 2011, **13**, 9655.
35 A. Ichihara and K. Yokoyama, *J. Chem. Phys.*, 1995, **103**, 2109.
36 A. Aguado, O. Roncero, C. Tablero, C. Sanz and M. Paniagua, *J. Chem. Phys.*, 2000, **112**, 1240.
37 H. Kamisaka, W. Bian, K. Nobusada and H. Nakamura, *J. Chem. Phys.*, 2002, **116**, 654.
38 W. Kutzelnigg and R. Jaquet, *Philos. Trans. R. Soc. London, Ser. A*, 2006, **364**, 2855.
39 L. P. Viegas, A. Alijah and A. J. C. Varandas, *J. Chem. Phys.*, 2007, **126**, 074309.
40 L. Velilla, B. Lepetit, A. Aguado, J. A. Beswick and M. Paniagua, *J. Chem. Phys.*, 2008, **129**, 084307.
41 R. A. Bachorz, W. Cenek, R. Jaquet and J. Komasa, *J. Chem. Phys.*, 2009, **131**, 024105.
42 T. Takayanagi, Y. Kurosaki and A. Ichihara, *J. Chem. Phys.*, 2000, **112**, 2615.
43 T. González-Lezana, A. Aguado, M. Paniagua and O. Roncero, *J. Chem. Phys.*, 2005, **123**, 194309.
44 R. F. Lu, T. S. Chu and K. L. Han, *J. Phys. Chem. A*, 2005, **109**, 6683.
45 F. J. Aoiz, V. Sáez Rábanos, T. González-Lezana and D. E. Manolopoulos, *J. Chem. Phys.*, 2007, **126**, 161101.
46 F. J. Aoiz, T. González-Lezana and V. Sáez–Rábanos, *J. Chem. Phys.*, 2007, **127**, 174109.
47 E. Carmona-Novillo, T. González-Lezana, O. Roncero, P. Honvault, J.-M. Launay, N. Bulut, F. J. Aoiz, L. Bañares, A. Trottier and E. Wrede, *J. Chem. Phys.*, 2008, **128**, 014304.
48 C. H. Zhang, W. Q. Zhang and M. D. Chen, *J. Theor. Comput. Chem.*, 2009, **8**, 403.
49 W. Q. Zhang and M. D. Chen, *J. Theor. Comput. Chem.*, 2009, **8**, 1131.
50 T. González-Lezana, P. Honvault, P. G. Jambrina, F. J. Aoiz and J.-M. Launay, *J. Chem. Phys.*, 2009, **131**, 044315.
51 A. Zanchet, O. Roncero, T. González-Lezana, A. Rodriguez-López, A. Aguado, C. Sanz-Sanz and S. Gómez–Carrasco, *J. Phys. Chem. A*, 2009, **113**, 14488.
52 P. G. Jambrina, F. J. Aoiz, C. J. Eyles, V. J. Herrero and V. Sáez Rábanos, *J. Chem. Phys.*, 2009, **130**, 184303.
53 W. Zhang, Y. Li, X. Chu and M. D. Chen, *Chem. Phys.*, 2010, **367**, 115.
54 P. G. Jambrina, F. J. Aoiz, N. Bulut, S. C. Smith, G. G. Balint-Kurti and M. Hankel, *Phys. Chem. Chem. Phys.*, 2010, **12**, 1102.
55 P. G. Jambrina, J. M. Alvariño, F. J. Aoiz, V. J. Herrero and V. Sáez Rábanos, *Phys. Chem. Chem. Phys.*, 2010, **12**, 12591.
56 T. P. Grozdanov and R. McCarroll, *J. Phys. Chem. A*, 2011, **115**, 6872.
57 E. Wrede, L. Schnieder, K. Seekamp-Schnieder, B. Niederjohann and K. Welge, *Phys. Chem. Chem. Phys.*, 2005, **7**, 1577.
58 H. Song, D. X. Dai, G. R. Wu, C. C. Wang, S. A. Harich, M. Y. Hayes, X. Y. Wang, D. Gerlich, X. M. Yang and R. T. Skodje, *J. Chem. Phys.*, 2005, **123**, 074314.
59 D. Dai, C. C. Wang, G. Wu, S. A. Harich, H. Song, M. Hayes, R. T. Skodje, X. Wang, D. Gerlich and X. Yang, *Phys. Rev. Lett.*, 2005, **95**(1), 013201.
60 D. Gerlich, *PhD thesis*, University of Freiburg, Germany, 1977.
61 D. Skouteris, J. F. Castillo and D. E. Manolopoulos, *Comput. Phys. Commun.*, 2000, **133**, 128.
62 M. Hankel, S. C. Smith, R. J. Allan, S. K. Gray and G. G. Balint-Kurti, *J. Chem. Phys.*, 2006, **125**, 164303.
63 M. Hankel, S. C. Smith, S. K. Gray and G. G. Balint-Kurti, *Comput. Phys. Commun.*, 2008, **179**, 569.
64 E. J. Rackham, T. González-Lezana and D. E. Manolopoulos, *J. Chem. Phys.*, 2003, **119**, 12895.
65 F. J. Aoiz, M. Brouard, C. Eyles, J. F. Castillo and V. Sáez Rábanos, *J. Chem. Phys.*, 2006, **125**, 144105.
66 *Gas Phase Ion Chemistry*, ed. M. T. Bowers, Academic Press, New York, 1979, vol. 1 and 2.
67 J. M. Farrar, in *Techniques for the study of ion–molecule reactions*, ed. J. M. Farrar and W. H. Saunders, Jr., J. Wiley & Sons, 1988.
68 C. Y. Ng and M. Baer, *State-selected and state-to-state ion–molecule reaction dynamics. Part 1. Experiment*, in *Adv. in Chem. Phys.*, Vol. LXXXII, 1992.
69 D. Gerlich, F. Windisch, P. Hlavenka, R. Plasil and J. Glosik, *Philos. Trans. R. Soc. London, Ser. A*, 2006, **364**, 3007.
70 D. Gerlich, in *Electronic and Atomic Collisions*, ed. D. C. Lorents *et al.*, Elsevier, Amsterdam, 1986, p. 541.
71 H. Kalmbach, *Diploma thesis*, University of Freiburg, Germany, 1989.
72 H. Gaber, *Diploma thesis*, University of Freiburg, Germany, 1987.
73 D. Gerlich and S. Horning, *Chem. Rev.*, 1992, **92**, 1509.
74 D. Gerlich, G. Borodia, A. Luca, C. Mogo and M. Smith, *Z. Phys. Chem.*, 2011, **225**, 475.
75 T. Warnock and R. Bernstein, *J. Chem. Phys.*, 1968, **49**, 1878.
76 D. Gerlich, *J. Chem. Phys.*, 1989, **90**, 127.
77 F. J. Aoiz, L. Bañares, V. J. Herrero, V. Sáez Rábanos, K. Stark and H.-J. Werner, *J. Chem. Phys.*, 1995, **102**, 9248.
78 W. Beyer, *Diploma thesis*, University of Freiburg, Germany, 1976.
79 T.-S. Chu, A. J. C. Varandas and K.-L. Han, *Chem. Phys. Lett.*, 2009, **471**, 222.
80 T.-S. Chu and K.-L. Han, *J. Phys. Chem. A*, 2005, **109**, 2050.